Thermal and lattice dynamical properties of Na_8Si_{46} clathrate

Liyan Qiu and Mary Anne White*
Department of Chemistry, Dalhousie University, Halifax, Nova Scotia, Canada B3H 4J3

Zhiqiang Li, John S. Tse, Christopher I. Ratcliffe, and Christopher A. Tulk
Steacie Institute for Molecular Sciences, National Research Council of Canada, Ottawa, Ontario, Canada K1A 0R6

Jianjun Dong
Physics Department, Auburn University, Auburn, Alabama 36849-5311

Otto F. Sankey
Department of Physics and Astronomy, and Materials Research Center, Arizona State University, Tempe, Arizona 85287-1504
(Received 30 October 2000; published 19 June 2001)

The experimental heat capacity of Na_8Si_{46} has been determined from 35–300 K, and its lattice parameters have been measured over the range 100–330 K. The experimental heat capacity and the thermal-expansion coefficient are compared with theoretical lattice-dynamical calculations for Na_8Si_{46}. The latter accurately reproduce the experimental thermal expansion and also give the first reliable assignment of the vibrational spectrum of this material, as judged by comparison of the calculated and experimental heat capacities. In addition, the theoretical results allow a calculation of the Grüneisen parameter of Na_8Si_{46}, which shows enhanced anharmonicity at low temperatures.

DOI: 10.1103/PhysRevB.64.024303 PACS number(s): 63.20.Ry, 63.50.+x, 65.40.Ba

I. INTRODUCTION

Inclusion compounds consist of two or more components in which one forms a host lattice with voids (cavities, channels, etc.) that can hold the other components (the guests). The intermolecular forces between the host and the guest usually are weak in comparison with chemical bonds. Clathrates are a subgroup of inclusion compounds in which the host forms cages to accommodate the guest species. Like most inclusion compounds, many clathrates require the presence of guest(s) to support the structure.

Silicon clathrates were first reported[1] in 1965. The two main structures of these materials are similar to type-I and type-II clathrate hydrates.[2] Silicon clathrates are stabilized with respect to the empty clathrate by the presence of metal atoms in the silicon-based cages. In both types of structure, each framework atom is sp^3 hybridized, forming covalent bonds with its nearest neighbors with a bond length and an energy only slightly greater than those in the crystalline diamond phase.[1,3] Theoretical studies show that the Si_{46} and Si_{136} structures have similar electronic properties[3,4] but these are quite different from the Si diamond structure. Since the metal atoms are located inside the cages formed by the framework atoms, silicon clathrates are chemically inert and do not react with air, moisture, or even strong acids except hydrofluoric acid.[1]

In the simple cubic structure type-I clathrate (general formula M_xSi_{46}, where M is a metal), there are 46 framework atoms in each unit cell, two small 20-atom cages, pentagonal dodecahedra $Si_{20}(I_h)$, and six large 24-atom cages, tetrakaidecahedra $Si_{24}(D_{6d})$. These solids are isostructural with gas hydrates such as $(Cl_2)_8(H_2O)_{46}$.[5] The metal atoms can be trapped in the pentagonal dodecahedra and in the tetrakaidecahedra. In M_xSi_{46}, the number of trapped metal atoms (these are usually alkali-metal and alkaline-earth metal atoms) depends on their size. If the metal atom is too big, only the larger cages are occupied and the small ones are empty.[6] When all the available cavities are occupied, the type-I clathrate has the ideal formula M_8Si_{46}.

The cages of silicon clathrates can be occupied by different metal atoms, giving mixed-metal-guest clathrates. Generally, smaller metal atoms (M) occupy the cages of Si_{20} and the larger ones (M') occupy the sites formed by Si_{24}.[7,8] When all the cages are completely occupied, with one metal in the smaller cages and another metal in the larger cages, the clathrate has the formula $M_2M'_6Si_{46}$. Metal atoms in the different cages can be clearly observed from solid-state NMR.[9]

The structure of the type-II clathrate is similar to, but distinct from, type I. In type II, 136 Si atoms form a face-centered-cubic structure that consists of sixteen smaller pentagonal dodecahedra (Si_{20}, I_h) and eight larger hexakaidecahedra (Si_{28}, T_d) in the unit cell.[6] The maximum guest occupancy is 24 per unit cell, $M_{24}Si_{136}$. The type-II semiconductor clathrates are isostructural with clathrate hydrates such as $(CCl_4)_8(H_2O)_{136}$ or $(H_2S)_{16}(CCl_4)_8(H_2O)_{136}$.[5]

Silicon clathrates can exhibit a variety of electronic behaviors. The electrical conductivity can be tailored from semiconductor to conductor by trapping different proportions of metal guest. Generally, M_8Si_{46} is metallic[10,11] and M_xSi_{136} is an insulator at low temperatures when $x<10$.[11] The precise electronic properties of Na_xSi_y clathrates depend on the guest occupancy, with Na primarily acting as an electron donor.[12] A similar conclusion was reached concerning K-doped Ge clathrates.[13] Recently, it was discovered that barium-doped Si clathrates show superconductivity below 10 K.[14,15] However, Na_8Si_{46} does not show superconductivity even at temperatures down to 2 K.[11]

The thermal conductivities of Si and Ge clathrates are much lower than that of their corresponding diamond phase below ambient temperatures[16] and resonant scattering via

dopant vibrations is suggested to explain the glasslike thermal conductivity, including that for Na_8Si_{46}.[12,16] The figure of merit, i.e., the utility of a thermoelectric material, depends on the dimensionless quantity ZT, where T is the absolute temperature and $Z=S^2\sigma/\kappa$, where S is the Seebeck coefficient, σ is the electrical conductivity, and κ is the thermal conductivity. Hence, the low thermal conductivities of Si clathrates could make them promising candidates for applications such as thermoelectric cooling and power generation.[16–18]

Heat capacity is one of the most fundamental thermal properties of a material. Accurate heat capacities are essential to calculate the thermodynamic functions ΔH, ΔS, and ΔG, from which thermodynamic stabilities can be assessed. Heat capacity also provides important information related to lattice dynamics and the understanding of anharmonic properties of lattice vibrations. In this paper, we report the heat capacity and related anharmonic properties of Na_8Si_{46}, from both experimental and theoretical approaches.

II. METHODOLOGICAL DETAILS

The heat capacity of Na_8Si_{46} was determined from 35–310 K, using an automated adiabatic calorimeter, which was operated in a heat-pulse mode.[19] The calorimeter had been tested previously with Calorimetry Conference standard benzoic acid, giving results that agreed with the literature to within 0.5%. The temperature was determined with a platinum resistance thermometer, which was calibrated according to ITS90.

A polycrystalline sample of Na_8Si_{46} of mass 0.9456 g was used for the calorimetric experiments. The rather large sample was prepared from combined batches from two preparations. The two samples were prepared by methods similar to those described previously.[20,21] A sodium silicide (NaSi) precursor was synthesized by reacting stoichiometric amounts of Na with Si in a stainless-steel vessel (evacuated and sealed) at 600 °C for 3 h. The air- and moisture-sensitive NaSi product was then wrapped in tantalum foil and placed in a Pyrex or quartz tube in an inert atmosphere dry box. This was heated in a furnace to 360 °C under active vacuum for 1 h. The tube was then closed under vacuum and heated at 445 °C or 430 °C for 20 h to produce Na_8Si_{46}. Na metal, from the decomposition of NaSi, condensed on the walls of the glass tube outside the furnace. The purity of the materials was determined by x-ray powder diffraction and ^{23}Na solid-state magic angle spinning NMR. ^{23}Na NMR, described elsewhere,[22] gave the characteristic spectrum of Na_8Si_{46} and showed no traces of Na metal or NaSi, to which the NMR is quite sensitive.

X-ray powder-diffraction patterns were measured using monochromatized Co Kα ($\lambda=1.790\,21$ Å) radiation on a Rigaku x-ray diffractometer (model RAD-R). For sample-purity analysis the data were collected over the range 5°–80° in 2Θ at 0.04° intervals in continuous scan mode at a scanning speed of 0.5°/min. The first sample contained traces of crystalline Si (estimated at $<1\%$) and the second sample had traces of Na_xSi_{136} (estimated at $<4\%$).

The lattice parameter of Na_8Si_{46} was determined using powder x-ray diffraction from two independent samples, at 11 temperatures between 90 and 330 K. The [222], [320], and [321] Bragg peaks were measured between 32–39° in 2Θ at intervals of 0.02° at a scan rate of 0.24°/min. The unit-cell size calculated using each peak individually was averaged at each temperature. For the thermal-expansion measurements crystalline silicon was included with the powdered samples to provide an internal reference.

Ab initio local-density approximation density-functional theory was applied to theoretically study the lattice dynamics of Na_8Si_{46}. Our calculations were performed with VASP,[23] which was implemented using ultrasoft pseudopotentials and plane-wave basis sets. The energy cutoff of the plane-wave basis was 150 eV, and the Brillouin-zone integration was numerically approximated using a $4\times4\times4$ k-point mesh. To determine lattice vibration eigenmodes and their frequencies, a direct approach of the force-constant matrix calculation was adopted. This approach has been applied to study the lattice dynamics of Si_{136},[24] Ge_{136}, and Ge_{46},[25] and results are in good agreement with available experimental data. The phonon spectrum was calculated using a primitive unit cell of Na_8Si_{46}, whose lattice constant was fixed. The equilibrium lattice constant was taken as 10.19 Å. The internal coordinates of the Na_8Si_{46} structure were optimized until a zero-force configuration was reached, i.e., all the atoms were at their equilibrium positions. Finally, the force-constant matrix was constructed by displacing each atom, one at a time, along one of three Cartesian directions with a small finite displacement (0.02 Å). A total of 162 ($=54\times3$) such displacements would be necessary to construct the full 162×162 force-constant matrix of Na_8Si_{46}. The highly symmetric cubic space group (Pm3n) coupled with group theory allowed us to significantly reduce the computational load to only nine such calculations. The lattice vibration eigenmodes and eigenfrequencies at the Brillouin-zone center (Γ point, $q=0$) were obtained by diagonalizing the force-constant matrix. Non-Γ-point ($q\neq0$) phonon modes can be approximated using this approach if the off-diagonal force constants between two neighboring atoms are assumed to decay to zero beyond a cutoff interatomic distance. The largest possible cutoff distance is half the lattice constant, which is believed adequate in this case due to the large unit cell and the fact that the force constants are indeed found to fall off rapidly with increased interatomic distance. The volume derivatives of the phonon frequencies necessary for calculation of the Grüneisen parameters were computed from the finite difference of two frequencies at neighboring volumes (volumes 10.12 and 10.19 Å, optimized at both).

III. RESULTS AND DISCUSSION

A. General features of the experimental heat capacity

The experimental heat-capacity results for Na_8Si_{46} (Fig. 1 and Ref. 26) show a smooth evolution of the heat capacity in this temperature range, indicating the presence of a single phase from $T=35-310$ K. The data smoothly approach the high-temperature limit of $54\times3R$ ($=1347\,\mathrm{J\,K^{-1}\,mol^{-1}}$).

Resulting thermochemical values [$(H\text{-}H(T=0\,\mathrm{K})$, $S\text{-}S(T=0\,\mathrm{K})$, $G\text{-}G(T=0\,\mathrm{K})$] (Ref. 26) indicate that the

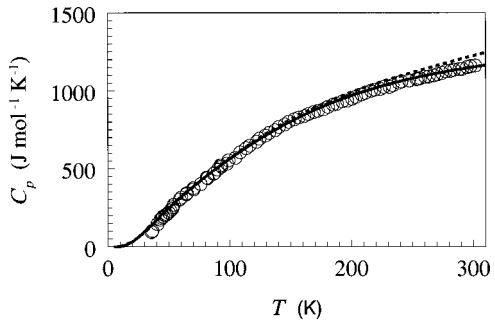

FIG. 1. Heat capacity of Na_8Si_{46}. Circles represent experimental data, dotted lines are the zone-center calculation with present vibrational assignment plus Debye modes plus empirical $(C_p - C_V)$ correction, and the solid line shows results of the full Brillouin-zone calculation.

standard entropy of formation of Na_8Si_{46}, derived from the entropies of the constituent elements[27,28] and of Na_8Si_{46}, is positive. (At $T=298.15$ K, $\Delta_f S^o$ is 32 ± 7 J K^{-1} mol^{-1}.) The positive entropy of formation decreases the Gibbs energy of formation and hence increases the thermodynamic stability of Na_8Si_{46}, with respect to the elements. Since the energy of silicon clathrates is thought to be higher than that of the diamond phase of Si (Ref. 29) the enthalpy of formation of silicon clathrates is expected to be positive. Hence, the positive value of $\Delta_f S^o$ is important in stabilizing the structure of silicon clathrates. Further quantitative calculation of $\Delta_f G^o$ requires additional experimental thermodynamic data such as the enthalpy of combustion.

B. Thermal expansion

The experimentally determined a lattice parameter of polycrystalline Na_8Si_{46} is shown as a function of temperature in Fig. 2.[26] The error bars represent twice the difference between the lattice constants as measured from the two independent samples. These data, in angstroms, were least-squares fit to a third-order polynomial in temperature (coefficients $a_0=10.181$, $a_1=-3.7\times10^{-5}$, $a_2=2.6\times10^{-7}$, $a_3=3.9\times10^{-10}$) in order to assess the linear thermal-expansion coefficient, $\alpha_a=\alpha_V/3=a^{-1}(\partial a/\partial T)_p$. For example, at $T=300$ K, the experimental data give $\alpha_a=2\times10^{-5}$ K^{-1}.

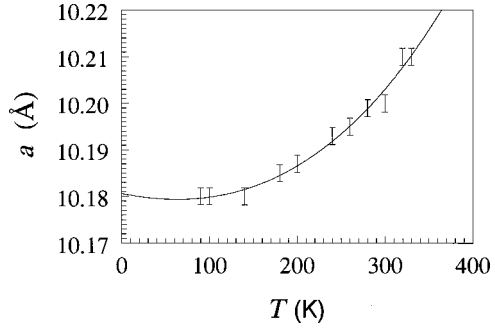

FIG. 2. Experimentally determined lattice parameters as a function of temperature, including experimental uncertainty. The solid line is a third-order polynomial least-squares fit to the data.

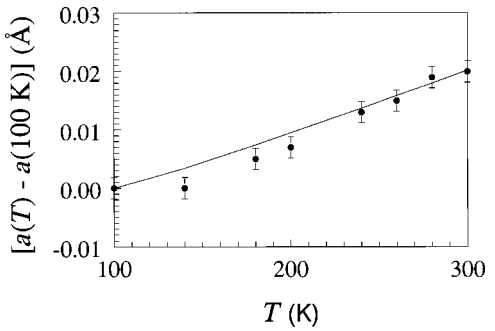

FIG. 3. The lattice parameter of Na_8Si_{46}, relative to its value at $T=100$ K, from experiment (data points and error bars) and the corresponding values from the theoretical approach (solid line).

From the theoretical perspective, the linear thermal-expansion coefficient can be written as

$$\alpha_a(T)=\frac{1}{3K}\sum_{q,n}\gamma_n(q)c_{\nu n}(q,T),$$

where K is the bulk modulus, $\gamma_n(q)$ is the mode Grüneisen parameter defined as

$$\gamma_n(q)=-\frac{d[\ln\omega_n(q,V)]}{d[\ln V]},$$

and $c_{\nu n}(q,T)$ is the mode contribution to the heat capacity,

$$c_{\nu n}(q,T)=\frac{\hbar\omega_n(q,V)}{V}\frac{d}{dT}\left[\exp\left(\frac{\hbar\omega_n(q,V)}{k_BT}\right)-1\right]^{-1}.$$

From our calculations, we determined the theoretical thermal expansivity as a function of temperature, from which we can assess the lattice parameter relative to that at a reference temperature. As shown in Fig. 3, the correspondence is excellent between the theoretical results for the increase in lattice parameter with temperature and the experimental data.

C. Analysis of the experimental heat capacity

The experimental heat capacity is that at constant pressure, i.e., C_p, but the more meaningful quantity to discuss lattice dynamics is C_V. For a cubic solid, these are related by $C_p-C_V=KTV(\alpha_V)^2$. Based on the present experimental results and the room-temperature experimental value of the bulk modulus[30] the difference between C_p and C_V is about 5% at room temperature, decreasing to a negligible difference (less than 0.1%) by about 100 K.

Comparison of calculated and experimental heat capacities can provide an excellent test of lattice-dynamical models. For Na_8Si_{46}, there are 54 atoms in the unit cell, and there should be $54\times3-3=159$ optic modes and 3 acoustic modes. There are several earlier reports of theoretical[4,31] and experimental[32–34] vibrational spectra of silicon clathrates, but the published theoretical frequencies are considerably higher than the experimental values. Furthermore, the modes had not been fully assigned; for example, of the 20 Raman lines

predicted for Na_8Si_{46} on the basis of group theory, 18 are associated with the Si framework, but only 15 have been observed experimentally.[32]

The assignment given in Table I is based on the theoretical investigation of the vibrational spectrum of Na_8Si_{46}. These vibration frequencies were used to calculate the optical contribution to the heat capacity of Na_8Si_{46}. To this we added an acoustic contribution for three modes with a Debye characteristic temperature of 371 K, deduced from the experimental density (see above) and the bulk modulus,[30] and a further term, based on the present lattice expansivity results, for $C_p - C_V$. (The optic contribution dominates, contributing more than 97% throughout the temperature range of the experimental results.) The resultant heat capacity is shown in Fig. 1. The match between these calculated values and the experiment is very good, in support of the vibrational assignment.

D. Comparison with theoretical heat capacity

The calculated heat capacity described above is essentially a zone-center calculation. A more accurate representation of the total theoretical heat capacity of the solid $C_V(T)$ would be from the sum of all modes over the Brillouin zone,

$$C_V(T) = \sum_{q,n} c_{\nu n}(q,T),$$

where again $c_{\nu n}(q,T)$ is the mode contribution to the heat capacity. The comparison of the theoretical and experimental heat capacity is shown in Fig. 1; the agreement is remarkably good, providing credibility for further use of this approach to quantify the anharmonicity of the interactions in Na_8Si_{46}.

E. Grüneisen parameter

Like the thermal-expansion coefficient and the thermal conductivity, the Grüneisen parameter γ can be used to quantify the anharmonic interactions within a lattice. Although the Grüneisen parameter γ for a vibration mode j can be calculated from its corresponding vibration frequency $\gamma_j = -(\partial \ln \nu_j / \partial \ln V)_T$, it is more convenient to calculate the overall γ from the more accessible experimental quantities with the equation $\gamma = \alpha_V V K / C_V$ for cubic phases. The relationship between γ_j and γ is given by $\gamma = \Sigma \gamma_j C_{\nu,j} / \Sigma C_{\nu,j}$, where $C_{\nu,j}$ is the heat capacity from mode j and the sum is over all vibration modes.

The experimentally determined value of γ is not accurately known below about $T = 150$ K, and even rather uncertain above this temperature, mostly because of uncertainty in the thermal-expansion coefficient. Nevertheless, it provides a useful check on the theoretically determined values of γ, and the agreement in the temperature range of overlap is good (see Fig. 4). The most interesting feature is the rather large increase in γ at low temperatures. A similar feature has been noted in other materials with reduced thermal conductivity (and enhanced anharmonicity), namely tetrahydrofuran clathrate hydrate[35] and Dianin's inclusion compound.[36] A similar behavior in γ has been observed[37] in CO and attributed to the existence of low-frequency librational modes.[38]

TABLE I. Vibrational assignments for Na_8Si_{46}. The values in brackets correspond to the experimental Raman spectra reported in Ref. 32. (NR)=mode not reported.

cm^{-1}	Symmetry	(R, Raman active; IR, Infrared active)	
0.0	T_{1u}		
57.0	T_{1g}		
57.9	T_{2g}	R	
58.2	T_{2u}		
62.1	T_{1u}	IR	
88.5	E_g	R	
89.3	T_{1u}	IR	
90.2	A_{2g}		
110.5	T_{2g}	R	(106.2)
121.0	T_{2u}		
121.2	T_{1u}	IR	
123.4	T_{1g}		
132.0	T_{1g}		
137.2	A_{2u}		
138.5	E_g	R	(123.1)
138.7	T_{2u}		
139.4	E_u		
139.7	T_{1u}	IR	
145.9	T_{1g}		
146.9	T_{2u}		
152.6	E_u		
158.8	T_{2g}	R	(129.8)
160.5	T_{1u}	IR	
161.5	T_{2g}	R	(138.1)
172.9	T_{1g}		
173.0	A_{2g}		
177.3	T_{1u}	IR	
203.0	E_g	R	(NR)
214.9	A_{2g}		
221.3	T_{2u}		
274.7	E_g	R	(255.9)
277.3	T_{2g}	R	(NR)
278.3	T_{1u}	IR	
295.9	T_{2u}		
310.1	A_{1u}		
310.5	A_{1g}	R	(313.1)
328.5	T_{1g}		
342.9	T_{2u}		
344.5	T_{1u}	IR	
352.2	A_{2g}		
356.8	A_{2u}		
379.5	E_g	R	(NR)
380.2	T_{1u}	IR	
382.0	T_{2g}	R	(328.9)
385.8	T_{1g}		
386.7	E_g	R	(338.1)
394.4	A_{1g}	R	(345.2)
398.5	T_{1u}	IR	
401.7	T_{2u}		
407.0	T_{2g}	R	(346.9)

TABLE I. (*Continued*.)

cm^{-1}	Symmetry	(R, Raman active; IR, Infrared active)	
407.8	E_u		
408.2	E_g	R	(378.4)
409.2	T_{2u}		
409.7	E_u		
411.2	T_{1u}	IR	
412.3	T_{1g}		
419.2	T_{1u}	IR	
419.4	T_{2u}		
420.9	T_{2g}	R	(405.3)
420.9	T_{1g}		
429.1	E_g	R	(415.6)
429.2	A_{1u}		
430.5	A_{2g}		
432.5	T_{2g}	R	(442.1)
432.7	T_{2u}		
436.4	A_{1g}	R	(453.8)

In Na_8Si_{46}, the unusual low-temperature anharmonicity can be associated with the low-frequency motions of the guests in the cages, resulting in very short mean free paths of the heat carriers, as shown by a recent analysis of the thermal conductivity and heat capacity.[39]

IV. CONCLUSIONS

The present theoretical investigations of thermal and associated lattice-dynamical properties of Na_8Si_{46} provide heat-capacity results that are in excellent agreement with experiment. In addition, they help assign the vibrational spectrum of Na_8Si_{46}. Furthermore, they provide strong evidence for low-frequency librational modes associated with motions of the guests in the cages, resulting in enhanced low-temperature anharmonicity and concomitantly reduced thermal conductivity in Na_8Si_{46} relative to pure Si.

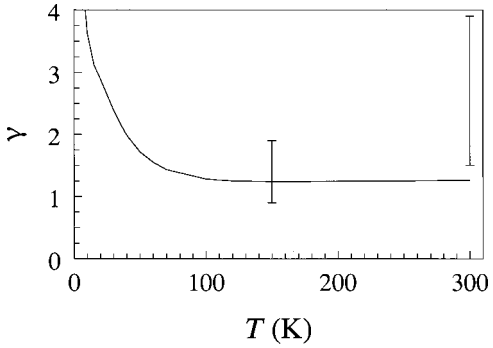

FIG. 4. Grüneisen parameter for Na_8Si_{46} as a function of temperature, from experiment (error bars, indicating uncertainty) and the theoretical analysis (solid line).

ACKNOWLEDGMENTS

The support to M.A.W. from the Natural Sciences and Engineering Research Council of Canada and the Killam Trusts is gratefully acknowledged.

*Author to whom correspondence should be addressed. Email address: Mary.Anne.White@dal.ca

[1] J. S. Kasper, P. Hagenmuller, M. Pouchard, and C. Cros, Science **150**, 1713 (1965).
[2] G. A. Jeffrey, in *Inclusion Compounds* (Academic, London, 1984), Vol. 1, pp. 135–190.
[3] G. B. Adams, M. O'Keeffe, A. A. Demkov, O. F. Sankey, and Y. Huang, Phys. Rev. B **49**, 8048 (1994).
[4] M. Menon, E. Richter, and K. R. Subbaswamy, Phys. Rev. B **56**, 12 290 (1997).
[5] J. A. Ripmeester, C. I. Ratcliffe, D. D. Klug, and J. S. Tse, Ann. N.Y. Acad. Sci. **715**, 161 (1994).
[6] E. Reny, P. Gravereau, C. Cros, and M. Pouchard, J. Mater. Chem. **8**, 2839 (1998); G. K. Ramachandran, P. F. McMillan, J. Dong, and O. F. Sankey, J. Solid State Chem. **154**, 626 (2000).
[7] F. Shimizu, Y. Maniwa, K. Kume, H. Kawaji, S. Yamanaka, and M. Ishikawa, Phys. Rev. B **54**, 13 242 (1996).
[8] S. Bobev and S. C. Sevov, J. Am. Chem. Soc. **121**, 3795 (1999).
[9] E. Reny, M. Menetrier, C. Cros, M. Pouchard, and J. Senegas, C. R. Acad. Sci., Ser. IIc: Chim. **1**, 129 (1998).
[10] C. Cros, M. Pouchard, and P. Hagenmuller, J. Solid State Chem. **2**, 570 (1970).
[11] S. Roy, K. E. Sim, and A. D. Caplin, Philos. Mag. B **65**, 1445 (1992).
[12] J. S. Tse, K. Uehara, R. Rousseau, A. Ker, C. I. Ratcliffe, M. A. White, and G. MacKay, Phys. Rev. Lett. **85**, 114 (2000); *ibid.* **86**, 4980 (2001).
[13] J. Zhao, A. Buldum, J. P. Lu, and C. Y. Fong, Phys. Rev. B **60**, 14 177 (1999).
[14] H. Kawaji, K. Iwai, S. Yamanaka, and M. Ishikawa, Solid State Commun. **100**, 393 (1996).
[15] R. F. W. Herrmann, K. Tanigaki, S. Kuroshima, and H. Suematsu, Chem. Phys. Lett. **283**, 29 (1998).
[16] J. L. Cohn, G. S. Nolas, V. Fessatidis, T. H. Metcalf, and G. A. Slack, Phys. Rev. Lett. **82**, 779 (1999).
[17] G. K. Ramachandran, J. Dong, J. Diefenbacher, J. Gryko, R. F. Marzke, O. F. Sankey, and P. F. McMillan, J. Solid State Chem. **145**, 716 (1999).
[18] F. J. DiSalvo, Science **285**, 703 (1999).
[19] M. J. M. Van Oort and M. A. White, Rev. Sci. Instrum. **58**, 1241 (1987).
[20] C. Cros, M. Pouchard, and P. Hagenmuller, Acad. Sci., Paris **260**, 4764 (1965).
[21] C. Cros and J.-C. Benejat, Bull. Soc. Chim. Biol. (Paris) **5**, 1739 (1972).
[22] J. He, D. D. Klug, K. F. Preston, C. I. Ratcliffe, K. Uehara, J. S. Tse, K. Uehara, and C. A. Tulk, J. Phys. Chem. B **105**, 3465 (2001).
[23] G. Kresse and J. Furthmuller, Comput. Mater. Sci. **6**, 15 (1996); Phys. Rev. B **54**, 11 169 (1996).

[24] J. Dong, O. F. Sankey, and G. Kern, Phys. Rev. B **60**, 950 (1999).
[25] J. Dong and O. F. Sankey, J. Phys.: Condens. Matter **11**, 6129 (1999).
[26] See EPAPS Document No. E-PRBMDO-64-064125 for the experimental lattice parameters, heat-capacity data, smoothed heat capacities, and associated thermochemical data [H-$H(T=0\ \mathrm{K})$, S-$S(T=0\ \mathrm{K})$, G-$G(T=0\ \mathrm{K})$]. This document may be retrieved via the EPAPS homepage (http://www.aip.org/pubservs/epaps.html) or from ftp.aip.org in the directory /epaps/. See the EPAPS homepage for more information.
[27] M. W. Chase and V. P. Itkin, J. Phys. Chem. Ref. Data **23**, 415 (1994).
[28] P. Flubacher, A. J. Leadbetter, and J. A. Morrison, Philos. Mag. **4**, 275 (1959).
[29] A. A. Demkov, O. F. Sankey, K. E. Schmidt, G. B. Adams, and M. O'Keeffe, Phys. Rev. B **50**, 17 001 (1994).
[30] A. San-Miguel, P. Kéghélian, X. Blase, P. Mélinon, A. Perez, J. P. Itié, A. Polian, E. Reny, C. Cros, and M. Pouchard, Phys. Rev. Lett. **83**, 5290 (1999); G. K. Ramachandran, P. F. McMillan, S. K. Deb, M. Somayazulu, J. Gryko, J. Dong, and O. F. Sankey, J. Phys.: Condens. Matter **12**, 4013 (2000).
[31] D. Kahn and J. P. Lu, Phys. Rev. B **56**, 13 898 (1997).
[32] S. L. Fang, L. Grigorian, P. C. Eklund, G. Dresselhaus, M. S. Dresselhaus, H. W. Kawaji, and S. Yamanaka, Phys. Rev. B **57**, 7686 (1998).
[33] Y. Guyot, B. Champagnon, E. Reny, C. Cros, M. Pouchard, P. Mélinon, A. Perez, and I. Gregora, Phys. Rev. B **57**, R9475 (1998).
[34] P. Mélinon, P. Kéghélian, A. Perez, B. Champagnon, Y. Guyot, L. Saviot, E. Reny, C. Cros, M. Pouchard, and A. J. Dianoux, Phys. Rev. B **59**, 10 099 (1999).
[35] J. S. Tse, J. Phys. Colloq. **48**, C1-543 (1987).
[36] M. Zakrzewski and M. A. White, J. Phys.: Condens. Matter **3**, 6703 (1991).
[37] E. K. Gill and J. A. Morrison, J. Chem. Phys. **45**, 1585 (1966).
[38] T. H. K. Barron, J. G. Collins, and G. K. White, Adv. Phys. **29**, 618 (1980).
[39] G. S. Nolas, J.-M. Ward, J. Gryko, L. Qiu, and M. A. White (unpublished).